PCCP

Azurin immobilisation on thiol covered Au(111)

O. Cavalleri,*[ab] C. Natale,[b] M. E. Stroppolo,[c] A. Relini,[ab] E. Cosulich,[d] S. Thea,[e] M. Novi[e] and A. Gliozzi[ab]

[a] Department of Physics, University of Genoa, Via Dodecaneso 33, 16146 Genoa, Italy.
E-mail: cavaller@fisica.unige.it; Fax: +39 010 314218; Tel: +39 010 3536087
[b] INFM Research Unit of Genoa, Genoa, Italy
[c] Department of Biology, University of Rome "Tor Vergata" and INFM Research Unit of Rome, Rome, Italy
[d] Department of Biochemistry, University of Pavia, Pavia, Italy
[e] Department of Chemistry and Industrial Chemistry, University of Genoa, Genoa, Italy

Azurin is a blue single copper protein involved in the respiratory chain of denitrifying bacteria. The structural gene for azurin from *Pseudomonas aeruginosa* was cloned in an *Escherichia coli* recombinant strain. The protein overexpressed in the bacterial periplasmic space was subsequently purified. Two strategies were followed to anchor azurin to gold surfaces. First, the protein was immobilised on bare gold. Azurin adsorbs on gold *via* its disulfide group. Scanning tunnelling microscopy (STM) inspection of the azurin–Au(111) interface revealed the formation of a closely packed protein monolayer and allowed individual azurin molecules to be resolved. In order to uncouple the protein layer from the metal, the gold surfaces were then covered with self-assembled monolayers of 11-mercaptoundecanoic acid. The changes in the sample morphology due to the protein adsorption have been investigated by atomic force microscopy (AFM). A fairly uniform distribution of protein molecules covers the surface. Owing to the tip broadening effect, an average protein diameter of about 20 nm was measured. An upper limit of 1 nN for the non-disruptive imaging force in the contact mode was found.

Introduction

In the 1980s, new technology requirements for chemically active materials led to the development of new techniques to bind organic molecules to the surface of inorganic substrates, thus allowing surface properties and functionalities to be tailored to a specific purpose. Self-assembly of organic monolayers to solid surfaces has proven to be a powerful method for the functionalisation of inorganic surfaces.[1-6] Among self-assembled monolayers (SAMs), the most widely studied systems have been SAMs formed by chemisorption of alkanethiols or disulfides on metal surfaces, such as Au, Ag or Cu.[7-9] Functional properties of these organic films are greatly improved when biomolecules, endowed with their own specific properties, are anchored at their surface. A major challenge is the development of strategies to assemble proteins into two-dimensional architectures ordered at the mesoscopic scale and able to accomplish specific functions such as molecular recognition, electron transfer or enzymatic activity.[10-17] In their natural environment, many proteins behave like transducers, converting chemical or physical signals into different ones. This makes these proteins very attractive for the fabrication of biosensors. The design of stable systems, which allow the immobilisation of enzymes on solid surfaces in such a way that they retain their activity unchanged, is still an open problem in the biotechnology field. A good immobilisation method should not only produce stable anchoring of active biomolecules, but should also result in reproducibly oriented bioassemblies. A number of different strategies, which take advantage of SAMs, have been developed for this purpose. These include genetic incorporation of functional coupling sites into protein structure,[13,14] fabrication of multi-layer systems (*e.g.*, SAMs from biotinylated thiols, streptavidin, biotinylated protein in turn),[10] formation of covalent bonds between suitable groups in the monolayer and functions in the protein. The last approach most commonly exploits the formation of amide bonds between carboxys of the SAM and free amino groups of the protein.[16-19]

We report here our first results on the immobilisation of azurin on bare and thiol covered gold surfaces. Azurin is a blue single copper protein with a molecular weight of 14 kDa consisting of 128 residues.[20] It acts as an electron transfer agent in the respiratory chain of denitrifying bacteria, where its role is to transport electrons between cytochrome c_{551} and cytochrome oxidase. It bears a disulfide bridge between two cysteines (Cys3Cys26) at its surface. The electron transfer centre is the Cu ion bound with His117, His46 and Cys112, which are almost coplanar. There are two other weak axial ligands binding the Cu ion, Met121 and Gly45. Two possible electron transfer pathways between the Cu centre and the disulfide bridge lying on the opposite side of the protein have been proposed.[21]

Experimental

Materials

Ethyl alcohol (99.9% pure), $HClO_4$ (70% puriss. p.a.) and $AcONH_4$ (5 M, BioChemika MicroSelect) were purchased from Fluka. 11-Bromoundecanoic acid (99%), *N*-hydroxysuccinimide (NHS) (97%), water-soluble carbodiimide (EDC) (98+%) and inorganic salts (ACS grade) used for buffers were obtained from Aldrich and used without further purification.

Buffers and solutions

Phosphate-buffered saline (PBS: 10 mM phosphate, 138 mM NaCl, 2.7 mM KCl, pH 7.4) and all the other solutions were prepared using water obtained from a Milli-Q purification system (Millipore, Bedford, MA, USA). AcONH$_4$ buffer (50 mM, pH 4.6) was prepared from the 5 M stock standard solution and the pH was adjusted with HClO$_4$ to the final value. The solution containing NHS and EDC was prepared immediately prior to use. Glassware was cleaned in Nochromix (Godax Laboratories, NY, USA) and thoroughly rinsed with Milli-Q water.

Sample preparation

Au(111) substrates. The gold substrates were prepared by vacuum evaporation of 99.99% pure gold up to a thickness of 140 nm onto preheated cleaved mica sheets. The evaporations were carried out at a base pressure of 2×10^{-6} mbar at a substrate temperature of 300–350 °C. Evaporations were followed by annealing under vacuum for 1–2 h up to 400 °C. Before use, the gold samples were annealed in a butane flame to glowing red and quenched in ethanol. STM inspections of the gold surface showed the presence of atomically flat (111) terraces, a few hundred nanometres in size, separated mostly by monoatomic steps. The samples for the self-assembly experiments were transferred into the appropriate solution immediately after quenching in order to minimise exposure to air.

11-Mercaptoundecanoic acid. 11-Mercaptoundecanoic acid was prepared from the corresponding bromide according to a method described previously for similar compounds.[22] The product, after purification by flash chromatography on silica gel (eluent: diethyl ether–light petroleum, 1 + 1), was characterised by ^{1}H NMR spectroscopy.

Azurin. The structural gene for azurin from *Pseudomonas aeruginosa* was isolated using oligonucleotides complementary to the amino and carboxy terminals of the *P. aeruginosa* azurin sequence. The 5′ amplification primer contained a *Hin*dIII restriction site upstream of the sequence and the 3′ amplification primer contained a *Sty*I restriction site in order to clone the amplified fragment into the expression vector pSE420 (Amp^R) (Invitrogen). Polymerase chain reaction (PCR) was carried out in 100 µL of reaction buffer containing 200 ng µL^{-1} of template DNA, 15 pM µL^{-1} of each primer, 2.5 mM dNTPs, 2.5 mM MgCl$_2$, 1 × running buffer and 1 unit of Taq polymerase (Boeringer). The amplified product was purified from agarose gel, digested with *Hin*dIII and *Sty*I and cloned into vector pSE420 (Amp^R) with a ligase reaction. The obtained expression plasmid pSE420–azurin was inserted by transformation into *Escherichia coli* recombinant strain 71/18.[23] DNA sequence analysis, performed using Sequenase (Bio-Rad Laboratories), confirmed that the expressed gene corresponded to that of *P. aeruginosa* azurin. Azurin was purified following a two-step protocol consisting of ion-exchange chromatography and gel filtration. *E. coli* cells were grown in 2 × YT medium supplemented with 50 µg mL^{-1} ampicillin as selective agent and (50 mM CuSO$_4$) at 37 °C for 17 h. Cells were then collected by centrifugation (12 800 rpm for 15 min at 4 °C) (Beckman centrifuge). The periplasmic fraction was obtained from the pellet following the method described by Karlsson *et al.*[24] The pH of the periplasmic fraction was adjusted to 4.1 with 0.5 M acetic acid and after incubation at 30 min at room temperature the precipitated proteins were separated from the clear supernatant containing azurin by centrifugation at 12 000 rpm for 20 min (BioFuge 17RS, Haereus Instruments, Hanau, Germany). All the subsequent steps were performed at 4 °C in a cold room.

For ion-exchange chromatography, the supernatant was loaded on a Whatman CM 52 column equilibrated with 0.05 M AcONH$_4$ (pH 4.1) and azurin was eluted with 0.05 M AcONH$_4$ (pH 5.1). A 2 µL mL^{-1} concentration of 0.5 M CuSO$_4$ was added to the fractions expected to contain azurin. The pooled fractions were then concentrated and loaded on a 1 m × 1.5 cm id Sephacryl S100 column (Pharmacia), previously equilibrated with 0.05 M AcONH$_4$ (pH 5.1). Proteins were eluted with 200 mL of the same buffer and azurin was detected by its blue color and by its absorbance at 625 nm. Positive fractions were then pooled, concentrated and stored at −20 °C. The homogeneity of the azurin containing fraction was checked by sodium dodecyl sulfate polyacrylamide gel electrophoretic analysis (SDS-PAGE) under reducing and non-reducing conditions. The protein (10 µg per lane) was loaded on a 12% polyacrylamide gel and after the run was stained with Coomassie Brilliant Blue.

SAMs. 11-Mercaptoundecanoic acid SAMs were prepared by keeping the freshly flame-annealed gold substrates in ethanolic thiol solutions (1 mM) for 12 h, after which they were removed, successively rinsed with ethanol and Milli-Q water and eventually transferred to the proper solution for subsequent protein deposition.

Protein layers

Azurin/Au(111). The azurin self-assembled monolayers were prepared by keeping the gold substrates in an azurin solution (0.5 mg mL^{-1} azurin in 50 mM AcONH$_4$, pH 4.6) at 4 °C for periods ranging from 1 to 3 days. After chemisorption, the samples were gently rinsed with AcONH$_4$ buffer, then dried in a nitrogen stream. Before analysis, the samples were exposed to vacuum for 30–45 min.

Protein/SAM/Au(111) immobilization procedure. SAM covered gold films were immersed for 30 min in a solution containing 0.05 M NHS and 0.2 M EDC in Milli-Q water. Samples were then rinsed with PBS and immersed for 2–12 h in the protein solution (0.5 mg mL^{-1} azurin in 50 mM AcONH$_4$, pH 4.6). The system was then rinsed with PBS and excess NHS esters were deactivated by washing for 10 min with pH 8.6 sodium phosphate buffer (25 mM). The films were finally rinsed with a solution of 50 mM AcONH$_4$ (pH 4.6).

Protein/SAM/Au(111) physical adsorption procedure. SAM covered gold films were immersed for 3–4 h in the protein solution (0.5 mg mL^{-1} azurin in 50 mM AcONH$_4$, pH 4.6). The film was then gently rinsed with a solution of 50 mM AcONH$_4$ (pH 4.6).

X-ray photoemission spectroscopy (XPS) measurements

XPS analysis was carried out with a PHI ESCA 5600 Multi-Technique electron spectrometer. The system consists of an X-ray Al-monochromatised source ($h\nu = 1486.6$ eV) and a spherical capacitor electron energy analyser, used in the fixed analyser transmission mode at a pass energy of 29.35 eV. In the standard configuration the analyser axis formed an angle of 45° with the sample surface.

Scanning probe microscopy measurements

The STM images were recorded with a Nanoscope II (Digital Instruments, Santa Barbara, CA) microscope equipped with a 0.45 µm scanning head. Tips were mechanically cut from 0.25 mm diameter Pt–Ir wire. The STM images were acquired in air at room temperature.

AFM measurements were performed in liquid with a Digital Instruments Dimension 3000 instrument equipped

with a G scanner head (92.8 μm scan range) and controlled by a Nanoscope III. AFM imaging was performed in the contact and tapping modes, the latter resulting in a less disruptive technique for the soft organic layers (see next section). Raw AFM data were processed by plane fitting. Standard Si_3N_4 triangular cantilevers (Digital Instruments) with a spring constant of 0.06 N m^{-1} were used. For the tapping mode, drive frequencies in the range 6–8 kHz, drive amplitudes in the range 16–20 V and set-points in the range 0.1–0.4 V were used.

Results and discussion

Azurin chemisorption on Au(111) surfaces

The formation of an azurin layer on the gold surfaces was checked by XPS. Fig. 1 shows an XPS survey spectrum of the azurin/Au(111) interface. The presence of N1s, C1s, O1s and S2p peaks in the XPS spectra of gold surfaces exposed to azurin solution qualitatively confirmed the deposition of azurin.

The azurin/Au(111) interface was characterised at the nanometer scale by STM in air. Fig. 2 compares the STM image of a bare Au(111) surface [Fig. 2(a)] with the STM image of the azurin/Au(111) interface [Fig. 2(b)]. Fig. 2(a) shows two gold terraces separated by a monoatomic step. On the upper terrace one can observe parallel rows of paired corrugations due to the herringbone reconstruction of the clean Au(111) surface.[25] Exposure of the gold substrate to the azurin solution results in the formation of a closely packed protein layer as shown in Fig. 2(b); two adjacent terraces decorated with a layer of bright spots are observed. As reported previously,[26-28] the disulfide bridge present on the protein outer shell is a suitable linker for the azurin self-assembly on the gold surface. Taking into account the three-dimensional structure of azurin[29,30] in which the disulfide bridge and the copper ion are located oppositely along the long molecular axis, the azurin SAM can be imagined as a dense layer of oriented molecules with the disulfide bridge bound to the gold surface and the copper ion facing up towards the outer SAM/gas interface. According to this model, an in-plane molecular cross-section of about 3×3 nm^2 is to be expected. The analysis of the STM images indicates the presence of round structures with diameters in the range 1.5–1.9 nm with an average centre-to-centre distance of about 3 nm.
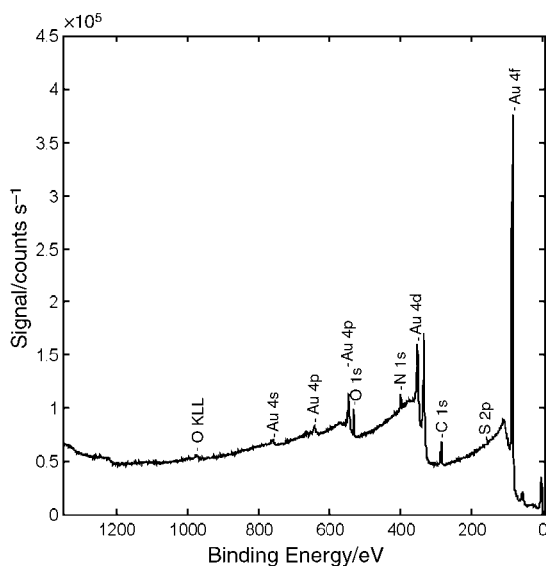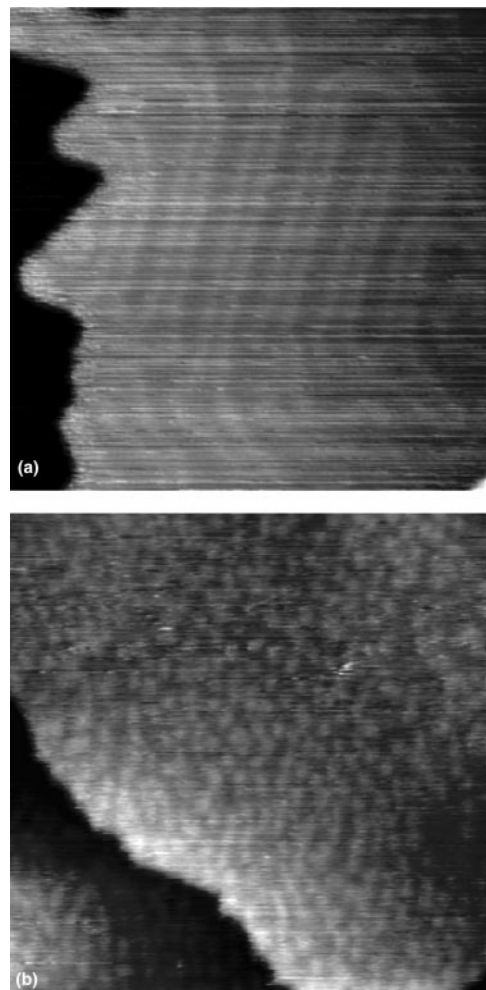

Fig. 2 (a) STM image of an Au(111) surface exhibiting the herringbone reconstruction. Image size: 55×55 nm^2. Tunnelling parameters: $I = 5.0$ nA, $V = 10$ mV. (b) STM image of the azurin/Au(111) interface. A distribution of bright spots, attributed to the tunnelling enhancement around the azurin copper ion, covers the surface. Image size: 60×60 nm^2. Tunnelling parameters: $I = 3$ nA, $V = 290$ mV.

The discrepancy between the diameter of the round spots and the in-plane azurin size could be explained by taking into account the origin of contrast in STM images. STM is not a topographical imaging tool and, except for some examples of homogeneous clean surfaces for which the STM images closely resemble the surface topography, the sample electronic structure has to be accounted for in the interpretation of the STM results.[31-33] The bright spots visible in the STM images of the azurin/Au(111) interface represent regions of high tunnelling currents conceivably due to enhanced tunnelling through the central part of each azurin molecule around the copper ion.

The average distance between the centres of adjacent spots is in agreement with the formation of a closely packed protein layer. The presence of a central region of higher current has also been observed with *in situ* STM imaging of the azurin/gold interface under potentiostatic control.[27]

Covalent azurin binding to thiol covered Au(111) surfaces

The covalent coupling of azurin to SAM-modified Au surfaces was obtained following a two-step procedure. The first step involved transformation of carboxys into *N*-hydroxysuccinimidyl ester functions, using the water-soluble coupling reagent EDC. Subsequently, coupling of these activated groups to protein amino groups was carried out. The combination of EDC and NHS is known to result in increased
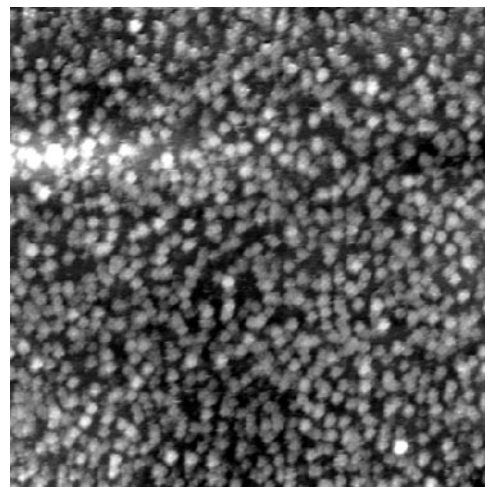

Fig. 1 XPS survey spectrum of the azurin/Au(111) interface.
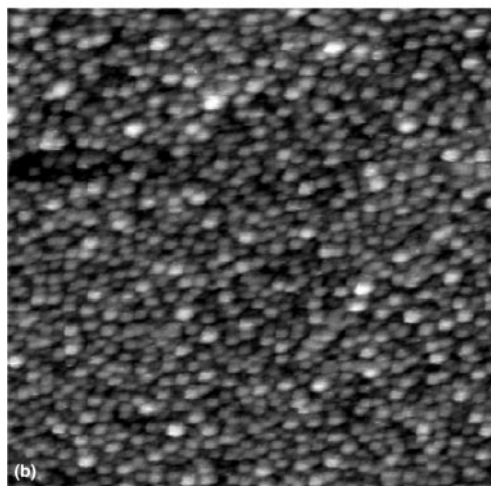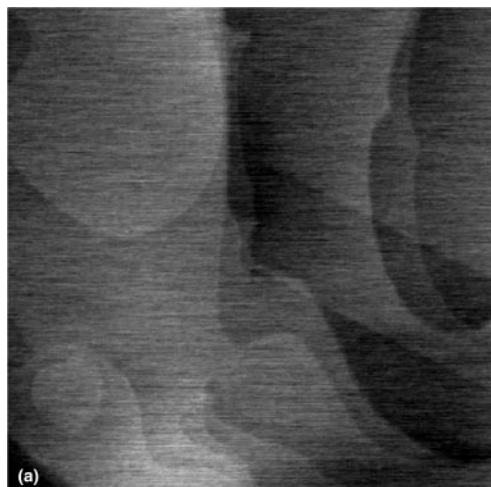
Fig. 3 Tapping mode AFM image of an 11-mercaptoundecanoic covered Au(111) surface. Image size: 1.5×1.5 μm². (b) Tapping mode AFM image of an azurin layer covalently bound to an 11-mercaptoundecanoic covered Au(111) surface. Image size: 650×650 nm².

yields of covalently coupled molecules.[17,19] Carbodiimide carboxylate activation leads to the formation of *O*-acylurea species which are known to undergo hydrolysis; *N*-hydroxysuccinimidyl esters, obtained by addition of NHS, are

Fig. 4 Contact mode AFM image of an azurin layer covalently bound to an 11-mercaptoundecanoic covered Au(111) surface. The disruptive effect of high force imaging can be observed in the middle of the imaged region. Image size: 2×2 μm².

Fig. 5 Tapping mode AFM image of an azurin layer physisorbed on an 11-mercaptoundecanoic covered Au(111) surface. Image size: 800×800 nm².

more stable molecules that allow a longer time interval for the formation of amide bonds in aqueous solution.

For the analysis of azurin layers on thiol covered gold surfaces, AFM, more suitable for the imaging of the relatively thick, poorly conductive organic layer, was preferred to STM. As discussed below, however, when imaging soft organic layers attention has to be paid to the imaging conditions because artefacts and sample damage can easily occur. As a basis for comparison we report in Fig. 3(a) the AFM image of an 11-mercaptoundecanoic acid SAM on Au(111) in 50 mM ammonium acetate (pH 4.6). Adjacent terraces, a few hundred nanometres in size, mostly separated by monoatomic height steps, are observed. The characteristic substrate holes present at the thiol/Au(111) interface[8,9,34,35] cannot be detected by AFM at this scale. Fig. 3(b) shows the image of an azurin film covalently bound to an 11-mercaptoundecanoic acid covered Au(111) surface in ammonium acetate buffer. A high surface density of proteins is observed. The azurin molecules have an apparent average diameter of about 20 nm. The diameters observed are significantly larger than the crystallographic data reported for azurin. This can be explained by taking into account the size of the AFM tip which has a typical radius of curvature of 20–60 nm. AFM images result from the convolution of the surface features with the tip shape,[36] causing the observed enhancement in the measured size. A similar effect has also been reported in previous *in situ* AFM studies on surface immobilised proteins.[37,38] Analysis of imaged proteins indicates a molecular height of about 4–5 nm. The measured z values are thus in agreement with the protein crystallographic size.

More care has to be taken in the interpretation of the molecular height when performing AFM in the contact mode. Whereas in the tapping mode the AFM probe is oscillating over the sample, thus avoiding continuous tip–surface contact, in the contact mode the probe is raster scanned over the sample in continuous contact with the surface. The sample is thus subject to lateral forces which can induce damage in soft organic samples. When imaging in the contact mode it is therefore necessary to minimise the loading force in order to reduce tip-induced sample modification.

The effect of non-optimised imaging conditions on the soft layer is illustrated in Fig. 4. The image was acquired in the contact mode with a force of 1 nN. Before recording the displayed image, a restricted portion of the surface was repeatedly scanned with forces of several nanonewtons. Damage is clearly visible in the image: whereas an almost uniform protein distribution is present in the region which has not been previously scanned, a disrupted layer with material clus-

tering and accumulation at the sides of the scanned area is clearly visible in the region which previously experienced high loads. Scanning the sample in the contact mode at different loading forces allowed us to find an upper limit to non-disruptive loads at about 1 nN. The evaluation of the protein height from contact mode images gives reliable results (about 3 nm) under low load (1 nN or less). The images acquired with higher forces show different surface topologies: molecules are either squeezed by the scanning tip, resulting in artificially thin and deformed features, or pushed laterally and aggregated into clusters with vertical dimensions between 10 and 30 nm, well above the molecular size.

At this stage of the work, no conclusive statement about the detailed mechanism of sample damage can be given. Taking into account the existence of a chemical bond between the protein and the thiol chain, it is conceivable that the whole thiol–protein ensemble is displaced by the scanning tip. Thiol displacement by the AFM tip has been observed in previous AFM studies, which investigated the reversible displacement of thiol molecules chemisorbed on gold obtained by increasing the loading force.[39,40]

Azurin physisorption on thiol covered Au(111) surfaces

Fig. 5 shows an AFM image of an azurin layer physisorbed on an 11-mercaptoundecanoic acid covered Au(111) surface in 50 mM ammonium acetate (pH 4.6). A fairly uniform distribution of protein molecules covers the surface. Similarly to covalently bound azurin (see above), the apparent in-plane dimensions of protein molecules (about 20 nm) exceed the actual size. When compared with the image in Fig. 3(b), the image in Fig. 5 reveals a lower protein surface density on the sample. However, some sample-to-sample variability was observed in the protein film density which, at this stage, does not allow us to make precise statements about protein density differences between covalently bound and physisorbed protein layers. The method used to anchor the protein to the SAM covered surface and also the thiol end-group (which controls the SAM affinity for proteins) can influence the layer density and structure.[41] We are currently carrying out measurements aimed at investigating this aspect, which is of great relevance for technological applications ranging from biosensors to biocompatibility research.

Conclusions

Azurin layers were deposited on both bare and thiol covered Au(111) surfaces. STM can successfully image the azurin/Au(111) interface with molecular resolution. STM inspection reveals a close packed layer of bright spots with an average centre-to-centre distance which fits well the in-plane azurin size (about 3 nm).

In order to avoid direct contact between protein and metal, azurin was then anchored to thiol covered Au(111) surfaces. Both physical adsorption and chemical binding lead to the formation of homogeneous layers which are stable for several days in their buffer solution. Tapping mode AFM was found to be a suitable tool for the non-disruptive imaging of the azurin/thiol/Au(111) interface with molecular resolution. A fairly uniform distribution of protein molecules with an average diameter of about 20 nm characterises the surface. The enlargement of the in-plane protein size is due to the tip broadening effect. Imaging loads below 1 nN allow reproducible and stable imaging of the soft layer, whereas increasing the force above this value results in layer disruption.

This work is the first step of a wider project aimed at producing ordered and preferentially oriented two-dimensional metalloprotein layers. One of the major aspects to be investigated is the relationship between electron transfer mechanism and protein orientation.

References

1 A. Ulman, *An Introduction to Ultrathin Organic Films: from Langmuir–Blodgett to Self-Assembly*, Academic Press, San Diego, 1991.
2 L. H. Dubois and R. G. Nuzzo, *Annu. Rev. Phys. Chem.*, 1992, **43**, 437.
3 H. O. Finklea, in *Electroanalytical Chemistry: a Series of Advances*, ed. A. J. Bard and I. Rubinstein, Marcel Dekker, New York, 1996, vol. 19, p. 109.
4 R. McKendry, M. E. Theoclitou, T. Rayment and C. Abell, *Nature (London)*, 1998, **391**, 566.
5 K. D. Schierbaum, T. Weiss, E. U. Thodem van Velzen, J. F. J. Engbersen, D. N. Reinhoudt and W. Göpel, *Science*, 1994, **265**, 1413.
6 F. Arias, L. A. Godinez, S. R. Wilson, A. E. Kaifer and L. Echegoyen, *J. Am. Chem. Soc.*, 1996, **118**, 6086.
7 F. Schreiber, A. Eberhardt, T. Y. B. Leung, P. Schwartz, S. M. Wetterer, D. J. Lavrich, L. Berman, P. Fenter, P. Eisenberger and G. Scoles, *Phys. Rev. B*, 1998, **57**, 12476.
8 C. Schönenberger, J. Jorritsma, J. A. M. Sondag-Huethorst and L. G. J. Fokkink, *J. Phys. Chem.*, 1995, **99**, 3259.
9 N. B. Larsen, H. Biebuyck, E. Delamarche and B. Michel, *J. Am. Chem. Soc.*, 1997, **119**, 3017.
10 J. Spinke, M. Liley, H.-J. Guder, L. Angermaier and W. Knoll, *Langmuir*, 1993, **9**, 1821.
11 S. Terrettaz, T. Stora, C. Duschl and H. Vogel, *Langmuir*, 1993, **9**, 1361.
12 I. Willner, M. Lion-Dagan, S. Marx-Tibbon and E. Katz, *J. Am. Chem. Soc.*, 1995, **117**, 6581.
13 M. A. Firestone, M. L. Shank, S. G. Sligar and P. W. Bohn, *J. Am. Chem. Soc.*, 1996, **118**, 9033.
14 J. Madoz, B. A. Kuznetzov, F. J. Medrano, J. L. Garcia and V. M. Fernandez, *J. Am. Chem. Soc.*, 1997, **119**, 1043.
15 B. A. Cornell, V. L. B. Braach-Maksvytis, L. G. King, P. D. J. Osman, B. Raguse, L. Wleczorek and R. J. Pace, *Nature (London)*, 1997, **387**, 580.
16 X. Su, F. T. Chew and S. F. Li, *Anal. Biochem.*, 1999, **273**, 66.
17 D. M. Disley, D. C. Cullen, H.-X. You and C. R. Lowe, *Biosens. Bioelectron.*, 1998, **13**, 1213.
18 G. J. Leggett, C. J. Roberts, P. M. Williams, M. C. Davies, D. E. Jackson and S. J. B. Tendler, *Langmuir*, 1993, **9**, 2356.
19 J. Lahiri, L. Isaacs, J. Tien and G. M. Whitesides, *Anal. Chem.*, 1999, **71**, 777.
20 A. G. Sykes, *Adv. Inorg. Chem.*, 1991, **36**, 377, and references cited therein.
21 O. Farver and I. Pecht, *Biophys. Chem.*, 1994, **50**, 203.
22 T. Zheng, M. Bukart and D. Richardson, *Tetrahedron Lett.*, 1999, **40**, 603.
23 T. Messing, B. Growenborc, B. Muller Hill and D. H. Hofshneider, *Proc. Natl. Acad. Sci. USA*, 1977, **74**, 3642.
24 B. G. Karlsson, T. P. Pascher, M. N. Nordling, R. H. A. Arvidsson and L. G. Lundberg, *FEBS Lett.*, 1989, **246**, 211.
25 J. V. Barth, H. Brune, G. Ertl and R. J. Behm, *Phys. Rev. B*, 1990, **42**, 9307.
26 E. P. Friis, J. E. T. Andersen, L. L. Madsen, N. Bonander, P. Møller and J. Ulstrup, *Electrochim. Acta*, 1997, **42**, 2889.
27 E. P. Friis, J. E. T. Andersen, Y. I. Kharkats, A. M. Kuznetsov, R. J. Nichols, J.-D. Zhang and J. Ulstrup, *Proc. Natl. Acad. Sci. USA*, 1999, **96**, 1379.
28 Q. Chi, J. Zhang, E. P. Friis, J. E. T. Andersen and J. Ulstrup, *Electrochem. Commun.*, 1999, **1**, 91.
29 H. Nar, A. Messerschmidt, R. Huber, M. van de Kamp and G. W. Canters, *FEBS Lett.*, 1992, **306**, 119.
30 M. van de Kamp, G. W. Canters, S. S. Wijmenga, A. Lommen, C. W. Hilbers, H. Nar, A. Messerschmidt and R. Huber, *Biochemistry*, 1992, **31**, 10194.
31 J. Tersoff and D. R. Hamann, *Phys. Rev. B*, 1985, **31**, 805.
32 H. Sumi, *J. Phys. Chem. B*, 1998, **102**, 1833.
33 N. J. Tao, *Phys. Rev. Lett.*, 1996, **76**, 4066.
34 G. E. Poirier and E. D. Pylant, *Science*, 1996, **272**, 1145.
35 O. Cavalleri, A. Hirstein and K. Kern, *Surf. Sci.*, 1995, **340**, L960.

36   D. Keller, *Surf. Sci.*, 1991, **253**, 353.
37   M. Fritz, M. Radmacher, J. P. Cleveland, M. W. Allersma, R. J. Stewart, R. Gieselmann, P. Janmey, Ch. F. Schmidt and P. K. Hansma, *Langmuir*, 1995, **11**, 3529.
38   F. Caruso, D. N. Furlong, K. Ariga, I. Ichinose and T. Kunitake, *Langmuir*, 1998, **14**, 4559.
39   S. Xu, P. L. Laibinis and G.-Y. Liu, *J. Am. Chem. Soc.*, 1998, **120**, 9356.
40   G.-Y. Liu and M. B. Salmeron, *Langmuir*, 1994, **10**, 367.
41   G. B. Sigal, M. Mrksich and G. M. Whitesides, *J. Am. Chem. Soc.*, 1998, **120**, 3464.